DE GRUYTER Nanotechnology Reviews 2021; 10: 1253–1265

Research Article

Zhenxia Li*, Tengteng Guo, Yukun Chen, Qi Liu, and Yuanzhao Chen

The properties of nano-$CaCO_3$/nano-ZnO/SBR composite-modified asphalt

https://doi.org/10.1515/ntrev-2021-0082
received August 9, 2021; accepted September 4, 2021

Abstract: To solve the problem of the pavement being aged due to the influence of temperature, light and other environmental factors are brought in service. Nano-$CaCO_3$ surface was activated by 6% KH-550, and nano-ZnO surface was activated by 6% aluminate. Nano-$CaCO_3$/nano-ZnO/SBR composite-modified asphalt was prepared. The optimum proportion of composite-modified asphalt was determined by orthogonal test. The influence of modifiers on asphalt pavement performance was comprehensively studied. The microstructure of composite-modified asphalt was characterized by scanning electron microscopy and infrared spectroscopy. The mechanism of composite-modified asphalt was analyzed. The results show that the optimum combination of composite-modified asphalt is 4% nano-$CaCO_3$ + 5% nano-ZnO + 4% SBR, the aging performance of the composite-modified asphalt is reduced by 6.9%, and the viscosity is increased by 14.6–23.1%. The complex shear modulus is increased by 24.1% at 82°C, the stiffness modulus is decreased, on average, by 21.1%. and the creep curve slope is increased by 9% on average. In the meantime, during the preparation process of composite-modified asphalt, it mainly occurred due to chemical reaction with surface-modified nanomaterials and physical change with SBR polymer materials.

Keywords: pavement material, modification mechanism, nanomaterials, composite-modified asphalt, microstructure

1 Introduction

With the emergence of complex road environment, increased traffic volume, and worsening climate and environment in recent years, it is difficult for asphalt pavement to meet the use requirements. Asphalt pavement is aging due to temperature, light, water, and ultraviolet radiation in the service process, which result in the decrease of low-temperature crack resistance of asphalt pavement and the decrease of asphalt elasticity, affecting its road performance [1]. Therefore, it has great significance to improve the physical properties and antiaging performance of asphalt by adding modifiers to meet the safety of modern traffic.

Polymers similar to waste rubber powder are often added as modifiers in traditional asphalt pavement, which can improve asphalt performance to a certain extent, but have side effects in terms of aging performance [2]. In recent years, nanomaterials have been gradually tried to be added to polymer-modified asphalt and rely on their special physical and chemical properties, or compounded in matrix asphalt by adding multidimensional materials and nanomaterials, such as nano-clay, carbon nanotubes, and nano-MMT are combined with SBR to modify asphalt [3–5]. It is found that nanoparticles are uniformly dispersed in the asphalt material when the nanomaterials are added to the asphalt, which can effectively improve the high-temperature stability, low-temperature crack resistance, fatigue resistance, anti-skid capability, aging resistance, durability, water stability, and construction workability of asphalt [6–10]. SBR, as a common modifier, swells under the action of saturates and aromatic in asphalt, reacts with organic functional groups in asphalt, and generates new chemical bonds, thereby improving the low-temperature crack resistance and bonding performance of asphalt [11–13]. The multi-effect of nano-$CaCO_3$ particles promotes the formation of strong van der Waals force with other molecules and forms a stable system. The high-temperature performance and aging resistance of asphalt are significantly improved by adding it [14–16]. Nano-ZnO shows superior performance in the field of optics, electricity, and magnetism. Adding nano-ZnO into

---

*** Corresponding author: Zhenxia Li,** School of Civil Engineering and Communication, North China University of Water Resources and Electric Power, Zhengzhou 450045, China,
e-mail: zhenxiali2009@ncwu.edu.cn
Tengteng Guo, Yukun Chen, Qi Liu, Yuanzhao Chen: School of Civil Engineering and Communication, North China University of Water Resources and Electric Power, Zhengzhou 450045, China

Open Access. © 2021 Zhenxia Li *et al.*, published by De Gruyter. This work is licensed under the Creative Commons Attribution 4.0 International License.

asphalt can effectively improve the aging performance and chemical resistance [17,18]. The test shows that nano-ZnO can be uniformly distributed in asphalt to form a space reticulate structure. With the increase of nano-ZnO content, the high-temperature performance and viscosity-temperature characteristics of modified asphalt are improved more obviously [19]. In summary, SBR can effectively improve the low-temperature crack resistance of asphalt. Nano-$CaCO_3$ improves the high-temperature performance of asphalt. Nano-ZnO not only helps to improve the high and low-temperature performance, but also plays a prominent role in antiaging and anti-fatigue performance.

Scholars have done a lot of research on improving the pavement performance of asphalt mixture and combined with mechanical software and computer simulation technology to carry out mechanical simulation analysis [20]. However, there are relatively few studies on the performance of asphalt alone and the improvement of its comprehensive performance. In addition, only a few scholars [21,22] have further explored the mechanism of asphalt modification. Thus, nano-$CaCO_3$/nano-ZnO/SBR composite-modified asphalt was prepared. The effects of modifiers on aging performance, viscosity, high-temperature performance, and low-temperature performance were studied. The microstructure of composite-modified asphalt was analyzed. The modification mechanism of each modifier was revealed. In this paper, a series of studies are carried out in order to obtain composite modified asphalt with better performance, the basis for its wide application in engineering practice in the future.

2 Raw materials

2.1 Asphalt

The asphalt used in this paper is the domestic AK-70 asphalt of Zhengzhou Municipal Engineering Corporation (Asphalt Pavement Co., Ltd). The macro performance index test of asphalt is carried out according to the test procedure (JTG E20–2011) [23]. The test results are shown in Table 1.

Table 1: Technical indicators of matrix asphalt

Index		Unit	Test results	Technical requirements
Penetration (25°C, 100 g, 5 s)		0.1 mm	61.5	60–80
Ductility (5 cm/min, 5°C)		cm	11.6	≥0
Softening point		°C	46.7	≥45
After TFOT	Quality change	%	0.327	−0.8 to +0.8
	Ductility (5°C)	cm	7.9	≥6
	Penetration ratio (25°C)	%	68.8	≥61

2.2 Nano-$CaCO_3$

Nano-$CaCO_3$ used in this paper is provided by Nanjing Epery Nanomaterials Co., Ltd, which is white powder; technical indicators are shown in Table 2.

2.3 Nano-ZnO

In this paper, the white powder nano-ZnO is provided by Nanjing Epery Nanomaterials Co., Ltd.; technical indicators are shown in Table 3.

2.4 SBR

SBR is provided by Tianjin Ming Fund Tai Rubber and Plastic Technology Co., Ltd., which is rice white powder; technical indicators are shown in Table 4.

3 Experimental

3.1 Preparation of composite-modified asphalt

3.1.1 Determination of optimum activation materials for nano-modifiers

The best coupling agent [24] is selected by comparison to conduct chemical modification on the surface of nanomaterials, which is conducive to better combination with asphalt. In this paper, KH-550, KH-570, and aluminate coupling agents were used to activate nanomaterials, and the best coupling agent was determined by lipophilicity test. Nano-$CaCO_3$ modification method was as follows: 10 g nano-$CaCO_3$ was weighed, and different doses of coupling agent solutions were configured. The mixed coupling agent solution was drained with a glass rod and added into three flasks. The electric stirrer was started for

Table 2: Technical indicators of nano-$CaCO_3$

Test items	Test results	Technical requirements
Quality fraction of $CaCO_3$ (%)	99.5	≥95
Average particle size of electron microscope (nm)	80	≤80
Specific surface area (m^2/g)	100	≥35
Volatiles at 105°C (%)	0.2	≤0.7

Table 3: Technical indicators of nano-ZnO

Test items	Test results	Technical requirements
Quality fraction of ZnO (%)	99.5	≥95
Average particle size of electron microscope (nm)	15	≤80
Specific surface area (m^2/g)	110	≥35
Volatiles at 105°C (%)	0.1	≤0.7

stirring at a constant speed of 100 rpm. Then, the nano-$CaCO_3$ was slowly added into three flasks to fully contact with the coupling agent solutions. The electric stirrer was adjusted to 300 rpm and stirred at a constant speed for 10 min after the addition of nano-$CaCO_3$, and then the heater was started up to 50°C and stirred for 20 min. After the stirring, the solutions were filtered out, and the remaining activated nano-$CaCO_3$ was put into an electric drying oven for drying. The temperature was controlled at 100°C. After drying, it was ground for use. Nano-ZnO modification method was as follows: Nano-ZnO was dried in a 100°C electric hot air dryer for 12 h. Different doses of coupling agent solutions were configured, stirred by glass rods for 10 min and then added to three flasks, using electric stirring motor, stirred at room temperature for 5 min. Then nano-ZnO was slowly added to the flask, and the motor temperature was adjusted to 60–80°C; the speed was adjusted to 300 rpm, stirring for 40 min. The activated nano-ZnO was placed in an electric drying oven, and the temperature was controlled at 105°C for drying. Finally, the dried nano-ZnO was placed in a mortar for grinding.

3.1.2 Preparation of nano-$CaCO_3$/nano-ZnO/SBR composite-modified asphalt

Adjust the temperature of heated asphalt to 80°C until all the asphalt melted for dehydration. After dehydration, a certain amount of matrix asphalt was weighed and placed on the heating base of a high-speed shear set at 135°C for no more than 30 min. In the heating process, glass rod was used to stir matrix asphalt to prevent asphalt aging due to local heating. The surface-modified nano-ZnO was added in the process of mixing. When it was integrated into asphalt, the high-speed shear was stabilized at 4,000 rpm and stirred for 15 min. After the high-speed stirring, the high-speed shear was adjusted to 1,500 rpm for stirring. At this time, the surface-modified nano-$CaCO_3$ was gradually added. After the addition was completed, the speed of the high-speed shear was adjusted to 4,000 rpm, and the stirring time was 15 min. After it was fully integrated into the asphalt, the shear was closed, and the sample was naturally cooled and placed for about 24 h. On the second day, the sample was reheated to about 135°C, and the speed was set at 1,500 rpm to add the required dose of SBR. After stirring until it was fully integrated into asphalt, the speed was set at 4,500 rpm, and continuous shear stirring was carried out for 25 min. After stirring, the rotational speed is adjusted to 1,500 rpm, and the SBR was sheared for 10 min, so that the SBR was further refined under low-speed shear stirring, and finally the composite-modified asphalt was prepared.

Combined with the personal test and previous scholars' summary [10,25] of the content test of the three modified materials in the matrix asphalt, the content of

Table 4: Technical indicators of SBR

Test items	Color	Particle size (purpose)	Dry rubber content (%)	Combinated styrene (%)
Technical requirements	Observation	GB/T2916	GB/T1040	GB/T8658
Test results	White	30	100	17–19

nano-$CaCO_3$ was finally determined to be 4, 5, and 6%, the content of nano-ZnO was determined to be 1, 3, and 5%, and the content of SBR was determined to be 3, 4, and 5%. The essential performance tests of nano-$CaCO_3$, nano-ZnO, and SBR with different doses were carried out. The optimal combination dosage of the three modifiers was obtained by orthogonal test [26]. Table 5 shows the dosage combination of each modifier in orthogonal test.

3.2 Thin film oven test

According to the T 0609-2011 in the test procedure (JTG E20-2011) [23], the composite-modified asphalt was prepared. The aging test of 50 g composite-modified asphalt heated for 5 h at 163°C was carried out to study the aging resistance of composite-modified asphalt.

3.3 Brookfield viscosity test

Since this paper mainly studies the viscosity of asphalt at different temperatures, the Brookfield viscometer method, namely the rotational viscosity test, was adopted. According to the T 0625-2011 in the test procedure (JTG E20-2011) [23], under the temperature conditions of 110, 120, 130, 135, 140, 150, 160, 175, 185, and 190°C, the viscosity tests of matrix asphalt and composite-modified asphalt were carried out to obtain the variation trend of viscosity and study the influence of modifiers on viscosity-temperature characteristics.

3.4 Dynamic shear rheological test

According to the T 0628-2011 in the test procedure (JTG E20-2011) [23], the test used a large sample of 25 mm diameter and 1 mm thickness for temperature scanning. The loading frequency was 10 rad/s, the control strain was 1%, the temperature range was from 46 to 82°C, and each interval was 6°C. The complex shear modulus G^*, phase angle δ, rutting factor $G^*/\sin\delta$ and other parameters of the matrix asphalt before and after aging, and the composite-modified asphalt before and after aging were tested by dynamic shear rheological to study the high-temperature performance of the composite-modified asphalt.

Table 5: The dosage combination of each modifier

Order number	Dosage (%)		
	Nano-$CaCO_3$	Nano-ZnO	SBR
1	4	1	3
2	4	3	4
3	4	5	5
4	5	1	4
5	5	3	5
6	5	5	3
7	6	1	5
8	6	3	3
9	6	5	4

3.5 Bending beam rheological test (BBR)

All kinds of asphalt were prepared into samples (147 mm long, 12.7 mm wide, 6.35 mm thick), at the test temperature of 12°C, 18°C, 24°C under zero by loading, unloading and constant load control, the matrix asphalt, composite modified asphalt bending rheological test, so as to determine the bending creep stiffness modulus S and creep curve slope m, study the low temperature crack resistance of asphalt.

3.6 Test of SEM

The field emission scanning electron microscope (SEM) with the model of JSM-7500F was used to test the four kinds of asphalt, namely, matrix asphalt, nano-$CaCO_3$-modified asphalt, nano-ZnO-modified asphalt, and SBR-modified asphalt. The distribution of single material in matrix asphalt can be compared and analyzed, and the microscopic observation of composite-modified asphalt can be carried out to distinguish the combination of the three materials with asphalt. In addition, through the analysis of the microstructure of these asphalts, the differences between them and the forces between various groups that may exist can be compared to determine whether the material and asphalt were chemically combined or physically combined.

3.7 Test of Fourier infrared spectrum

The infrared spectrum test and scanning analysis are carried out by the frontier Fourier infrared spectrometer, in which the wave number range is 4,000–400/cm, the resolution is 4/cm, and the scanning times are 64. The modification effect of coupling agent on nanomaterials

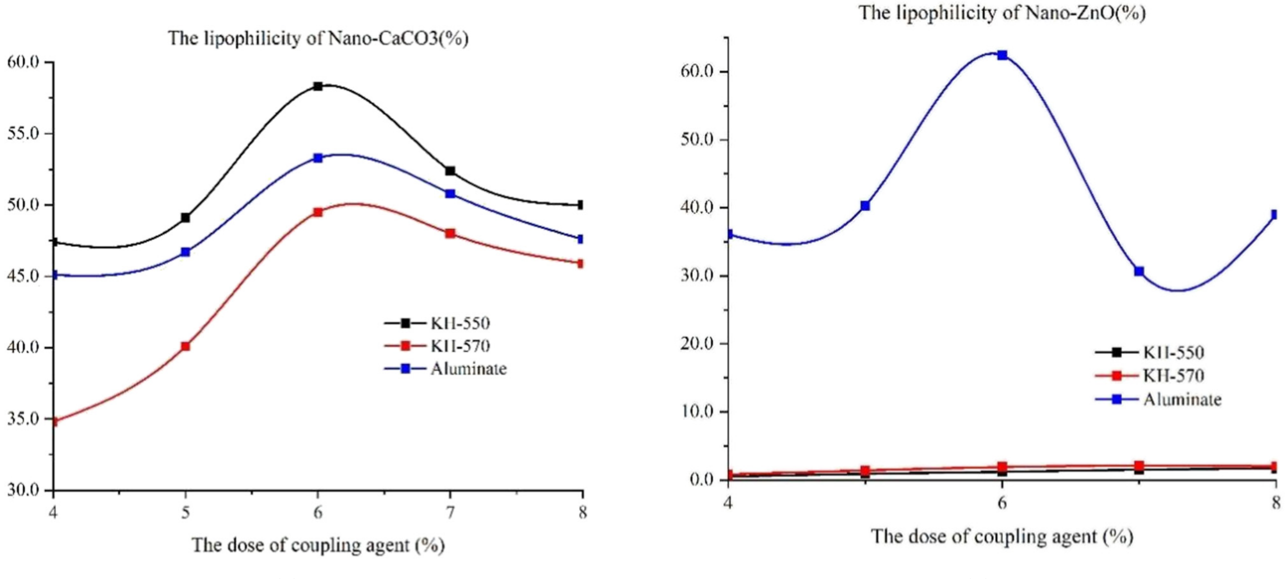

(a) (b)

Figure 1: Lipophilic degree of activated nanomaterials: (a) lipophilic degree of activated nano-$CaCO_3$ and (b) lipophilic degree of activated nano-ZnO.

and the reaction process with nanomaterials during the preparation of composite-modified asphalt were determined.

4 Test results and analysis

4.1 Optimum coupling agent and dosage of nanomaterials

Three kinds of coupling agents, KH-550, KH-570, and aluminate, were used to activate the surface of nanomaterials, and the best coupling agent and its dosage were determined by lipophilicity test. It can be seen from Figure 1 that the activation effect of KH-550 on nano-$CaCO_3$ is better than that of KH-570 and aluminate, and the optimal dose is 6%. The activation effect of aluminate on nano-ZnO is better than that of KH-550 and KH-570, and the optimal dose is also 6%. Therefore, 6% KH-550-activated nano-$CaCO_3$ and 6% aluminate-activated nano-ZnO are finally selected.

4.2 Determination of optimum dosage combination

The penetration test, ductility test, and softening point test were carried out according to the dosage combination of each modifier in the orthogonal test determined in 3.2. Finally, the range analysis method was used to analyze the results of the orthogonal test, as shown in Table 6.

According to the penetration index, the optimal proportion results are: nano-$CaCO_3$ content is 4%, nano-ZnO content is 5%, and SBR content is 5%. According to the softening point index, the optimal proportion results are: nano-$CaCO_3$ content is 4%, nano-ZnO content is 3%, and SBR content is 4%. According to the ductility index, the optimum proportion results are: nano-$CaCO_3$ content is 5%, nano-ZnO content is 5%, and SBR content is 4%. Considering the comprehensive balance method and economy, nano-$CaCO_3$ mainly affects the high-temperature performance of asphalt, and the content of nano-$CaCO_3$ is determined to be 4%. Nano-ZnO has a great influence on the aging resistance, and the content of nano-ZnO is determined to be 5%. SBR is the best to improve the low-temperature performance of asphalt, and the SBR content is 4%. Finally, the best combination dosage is: 4% nano-$CaCO_3$ + 5% nano-ZnO + 4% SBR.

4.3 Analysis of aging performance

The performance test results of matrix asphalt and modified asphalt before and after aging are shown in Table 7. The mass loss of matrix asphalt under short-term aging condition of thin film heating oven is 0.327%, and the mass loss of composite-modified asphalt is 0.101%.

Table 6: Range calculation results of orthogonal experiment

Test items	Nano-$CaCO_3$	Nano-ZnO	SBR
(25°C, 100 g, 5 s) Penetration (0.1 mm)			
*K*1	136.9	139.8	140.1
*K*2	143.2	151.6	143.9
*K*3	142.1	130.8	132.3
*k*1	45.6	49.6	46.7
*k*2	47.7	51.5	47.9
*k*3	47.4	43.6	44.1
Extreme difference	2.1	7.9	3.8
Optimization	4%	5%	5%
Softening point (°C)			
*K*1	159.8	156.7	158.2
*K*2	158.1	159.6	158.9
*K*3	156.8	158.4	157.6
*k*1	53.3	52.3	52.7
*k*2	52.7	53.2	53.0
*k*3	52.3	52.8	52.5
Extreme difference	1.0	0.9	0.5
Optimization	4%	3%	4%
(5 cm/min, 5°C) Ductility (cm)			
*K*1	42.3	42.1	42.2
*K*2	42.4	41.2	43.2
*K*3	41.0	42.4	40.3
*k*1	14.1	14.0	14.1
*k*2	14.1	13.7	14.4
*k*3	13.6	14.1	13.4
Extreme difference	0.5	0.4	1.0
Optimization	5%	5%	4%

Note: The value of *K* represents the total value of each factor at each level. The value of *k* represents the average value of the total value, and the value indicates the influence of this factor on the test parameters.

From the test results of residual penetration ratio, the residual penetration ratio of matrix asphalt is 68.8%, the residual penetration ratio of composite-modified asphalt is 79.4%, and the residual penetration ratio of composite-modified asphalt is 15.4% higher than that of matrix asphalt. Through the ductility test, the ductility value of matrix asphalt after aging is 31.9% lower than that before aging, and the ductility value of composite-modified asphalt is 6.9% lower than that before aging, which shows that composite-modified asphalt can slow down the decrease of ductility value. It indicates that the addition of modifiers reduces the mass loss of matrix asphalt and increases the residual penetration ratio, which can effectively prevent asphalt aging and improve the antiaging performance.

4.4 Analysis of Brookfield viscosity test

According to the 3.5, the viscosity test of matrix asphalt and composite-modified asphalt was carried out. The test results are shown in Figure 2. It can be seen that with the increase of temperature, the viscosity decreases gradually, but on the whole, the viscosity of the composite-modified asphalt is 14.6–23.1% higher than that of the matrix asphalt. Additionally, it can be seen that when the temperature is 135°C, the viscosity value of the composite-modified asphalt does not exceed 3 Pa·s, which is beneficial to the construction. Therefore, the viscosity of composite-modified asphalt is better. The increase of viscosity can enhance the ability of asphalt to resist shear deformation when it is added to the mixture, and its ability to resist rutting is also increased. It shows that the addition of modifiers can improve the high-temperature performance of asphalt and also has good construction performance.

4.5 Analysis of rheological property

4.5.1 Dynamic shear test results

According to the test method mentioned in 3.6, dynamic shear tests were carried out on four samples, and the

Table 7: Short-term aging test results of modified asphalt

Asphalt type	Before aging			After aging			
	Mass (g)	25°C penetration (0.1 mm)	Ductility (cm)	Mass loss (%)	25°C penetration (0.1 mm)	Residual penetration ratio (%)	Ductility (cm)
70 # asphalt	49.851	61.5	11.6	0.327	42.3	68.8	7.9
Composite-modified asphalt	50.066	50.3	25.9	0.101	39.9	79.4	24.1

results are shown in Figure 3. It shows that the complex shear modulus decreases and the phase angle increases with the increase of temperature before asphalt aging. When the temperature rises to 70°C, the value of matrix asphalt rutting factor $G^*/\sin\delta$ is 0.94 kPa, which is less than ≥1.0 kPa required by the test procedure (JTG E20-2011) [23]. On the contrary, the rutting factor $G^*/\sin\delta$ of composite-modified asphalt at 82°C is 1.14 kPa. Therefore, adding modifiers in asphalt can effectively resist rutting deformation, indicating that the addition of composite-modified materials improves the high-temperature performance of asphalt.

After asphalt aging, the complex shear modulus G^* of matrix asphalt and composite-modified asphalt gradually decrease with the increase of temperature, but at the same temperature, the complex shear modulus of composite-modified asphalt after aging is greater than that of matrix asphalt after aging. It illustrates that the shear deformation resistance of aged composite-modified asphalt is stronger than that of aged matrix asphalt. The phase angle of matrix asphalt and composite-modified asphalt after aging is smaller than that before aging, because the viscous and elastic components inside the matrix and composite-modified asphalt after aging are decreased, and the asphalt is slowly hardened, resulting in the decrease of phase angle. However, it is found that the phase angle of the aged composite-modified asphalt is smaller than that of the aged matrix asphalt, indicating that the elastic recovery ability of the modified asphalt is stronger than that of the matrix asphalt in the subsequent service process.

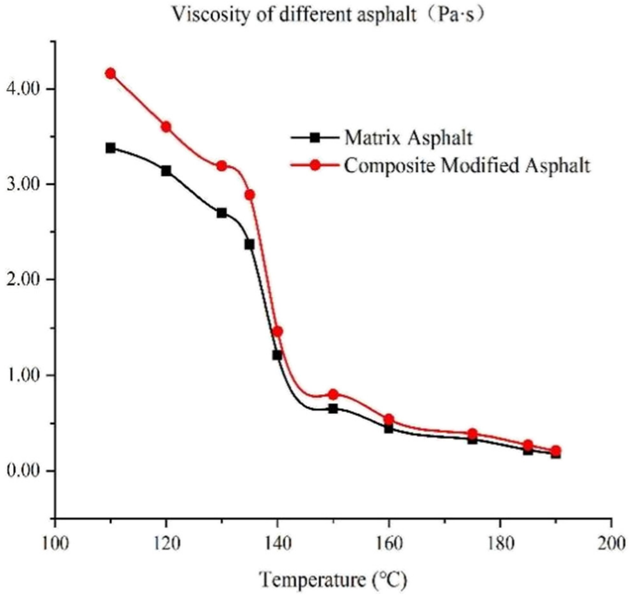

Figure 2: Results of Brookfield viscosity test.

The rutting factor $G^*/\sin\delta$ of aged asphalt at 82°C is 0.84 kPa, while the rutting factor $G^*/\sin\delta$ of aged composite-modified asphalt at 82°C is 1.03 kPa, which is greater than ≥1.0 kPa required by T 0628-2011 in the test procedure (JTG E20-2011) [23]. It also reveals that the addition of modifiers can effectively slow down the rutting deformation and enhance the ability to resist rutting in short-term use.

In conclusion, the addition of modified materials can effectively resist rutting deformation and improve the high-temperature performance of asphalt.

4.5.2 Bending beam rheological test results

The bending beam rheological test results of matrix asphalt and modified asphalt are shown in Table 8. It can be seen that with the decrease of temperature, the stiffness modulus S values of composite-modified asphalt are smaller than that of matrix asphalt, and the decrease ratios are 15.6, 30.5, and 17.3% under three temperature conditions. Consequently, the addition of modifiers improves the relaxation ability of matrix asphalt at low temperature and improves the low-temperature crack resistance of asphalt. From the slope m values of creep curve, the m values of

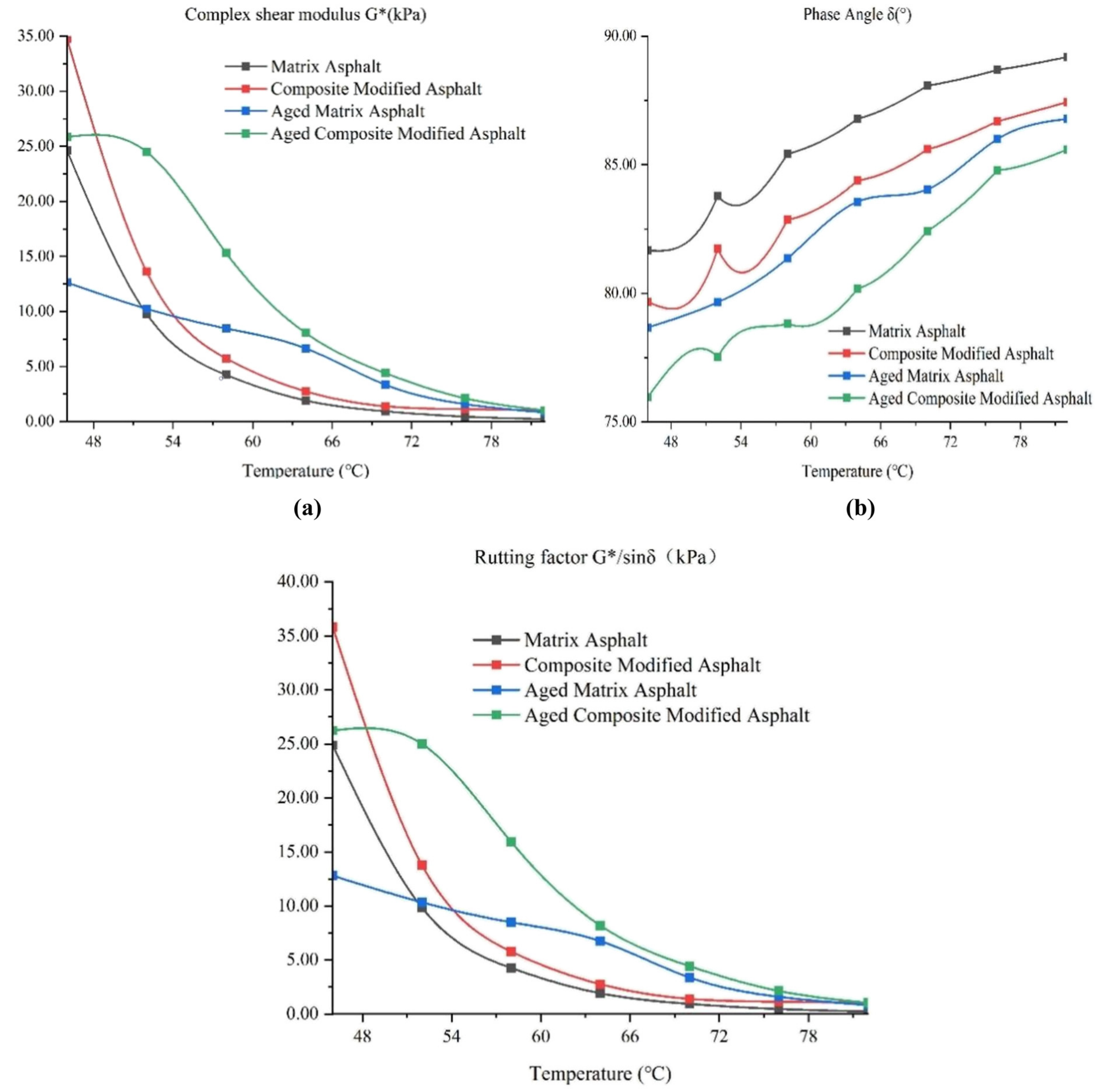

(a)

(b)

(c)

Figure 3: Different asphalts dynamic shear test results. (a) Different asphalts complex shear modulus, (b) different asphalts phase angle, and (c) different asphalts rutting factor.

Table 8: Freeze-thaw test results of cement stabilized gangue mixture

Asphalt type	Creep stiffness modulus S (MPa)			Creep curve slope m		
	−12°C	−18°C	−24°C	−12°C	−18°C	−24°C
70 # Asphalt	101.4	275.0	649.0	0.401	0.307	0.247
Composite-modified asphalt	85.7	191.0	537.0	0.442	0.335	0.266

matrix asphalt and composite-modified asphalt gradually decrease with the decrease of temperature, and the m values of composite-modified asphalt are larger than that of matrix asphalt. However, compared with the matrix asphalt, the composite-modified asphalt increases by 10.2, 9.1, and 7.8% at different temperatures. It shows that modifiers are not easy to produce tensile stress due to temperature shrinkage deformation under low-temperature conditions. The addition of modifiers can improve the low-temperature crack resistance of asphalt.

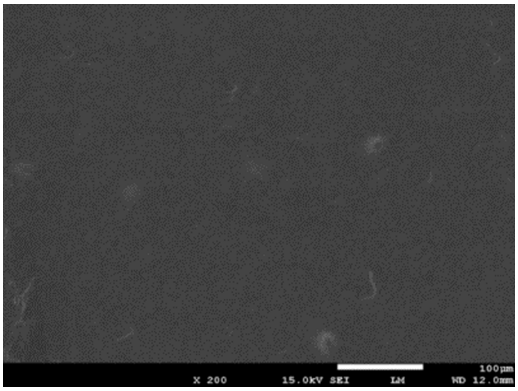

Figure 4: Image of matrix asphalt.

4.6 Analysis of composite asphalt morphological characterization

4.6.1 Morphology characterization of matrix asphalt

Matrix asphalt is amplified 200 times image as Figure 4, there are no other substances or particles in the image, and the image surface is smooth and uniform.

4.6.2 Morphology characterization of nano-CaCO$_3$-modified asphalt

The partial amplification of nano-CaCO$_3$-modified asphalt is 5,000 times as shown in Figure 5(a). It can be seen that there is a small amount of agglomeration in the figure, which also reflects that the effect of high-speed shear used in the early stage to modify nanomaterials does not reach 100%. But when amplifying another local nano-CaCO$_3$-modified asphalt 10,000 times, as shown in Figure 5(b), it is found that it is uniformly dispersed in asphalt and some are wrapped in asphalt. Because of some characteristics of nanoparticles, the active particles are combined with the molecules in the asphalt to form a relatively stable network structure, which also makes the nano-CaCO$_3$ particles form a continuous phase with the asphalt molecules, increasing the overall structure resistance to load and improving the thermal stability.

4.6.3 Morphology characterization of nano-ZnO-modified asphalt

The local amplification of nano-ZnO-modified asphalt is 2,000 times as Figure 6(a). It can be seen that there is a small amount of agglomeration in the figure, but the overall dispersion effect is still good. When amplifying another local nano-ZnO-modified asphalt 10,000 times, as shown in Figure 6(b), nano-ZnO is uniformly dispersed in asphalt and nano-ZnO and asphalt form a network structure, which may be due to the high-speed stirring of high-speed shear machine to destroy the structure of nano-ZnO particles, increase the surface activity of particles, and make it more closely combined with the asphalt interface. The destruction of nano-ZnO particles changes the chemical structures such as functional groups and covalent bonds and enhances the viscosity and toughness of modified asphalt, thereby improving the performance of asphalt.

4.6.4 Morphology characterization of SBR-modified asphalt

The two images in Figure 7 are amplified by 5,000 and 10,000 times of SBR-modified asphalt. It can be found that SBR is evenly distributed in asphalt which is due

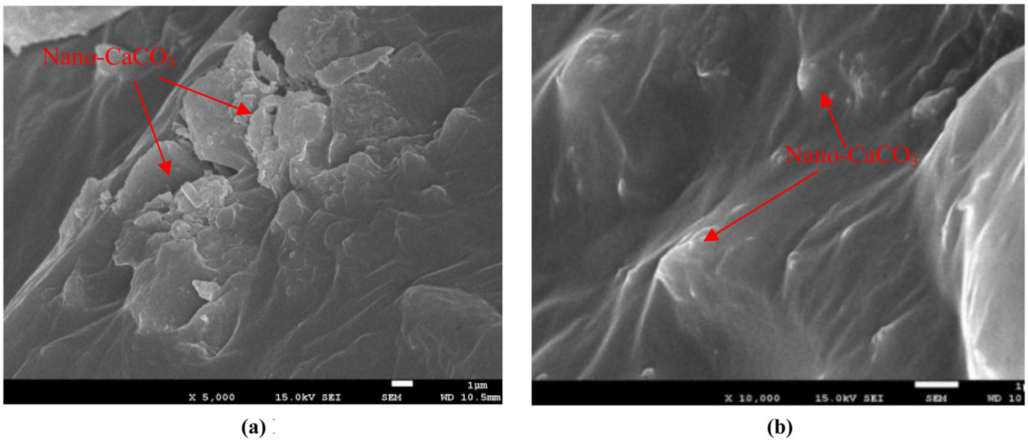

Figure 5: Different magnification images of nano-CaCO$_3$-modified asphalt: (a) nano-CaCO$_3$-modified asphalt amplifies 5,000 times and (b) nano-CaCO$_3$-modified asphalt amplifies 10,000 times.

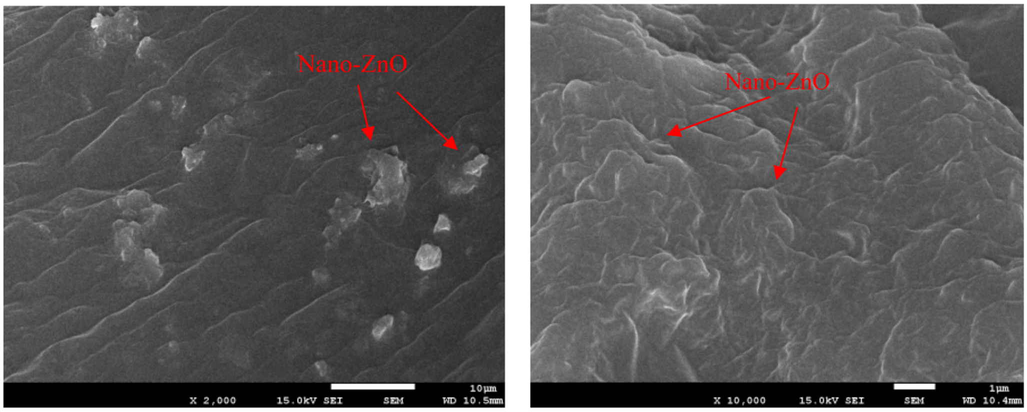

(a) (b)

Figure 6: Different magnification images of nano-ZnO-modified asphalt: (a) nano-ZnO-modified asphalt amplifies 2,000 times and (b) nano-ZnO-modified asphalt amplifies 10,000 times.

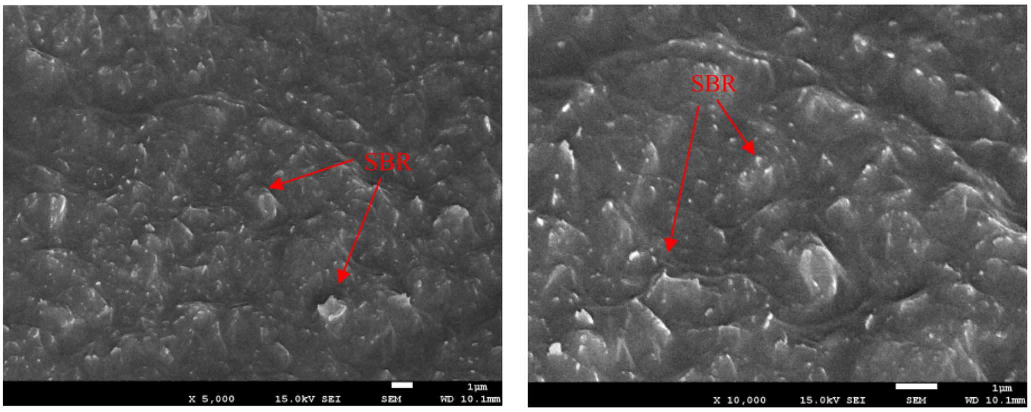

(a) (b)

Figure 7: Different magnification images of SBR-modified asphalt. (a) SBR-modified asphalt amplifies 5,000 times and (b) SBR-modified asphalt amplifies 10,000 times.

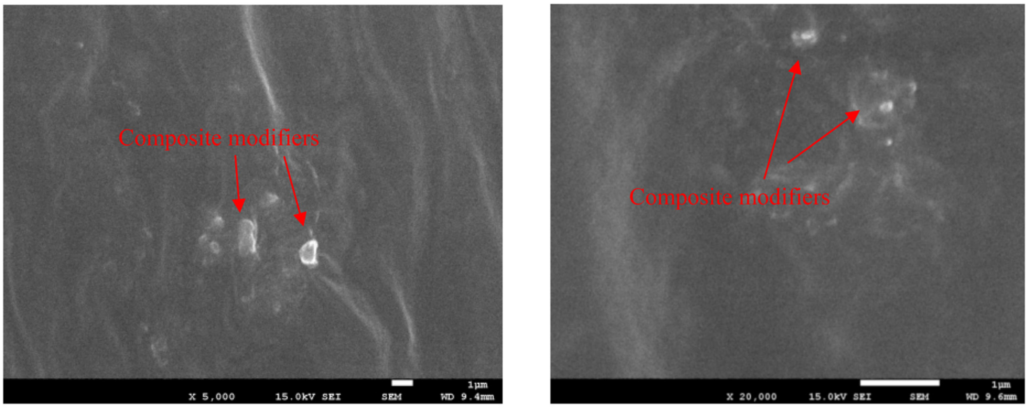

(a) (b)

Figure 8: Different magnification images of composite-modified asphalt: (a) composite-modified asphalt amplifies 5,000 times and (b) composite-modified asphalt amplifies 20,000 times.

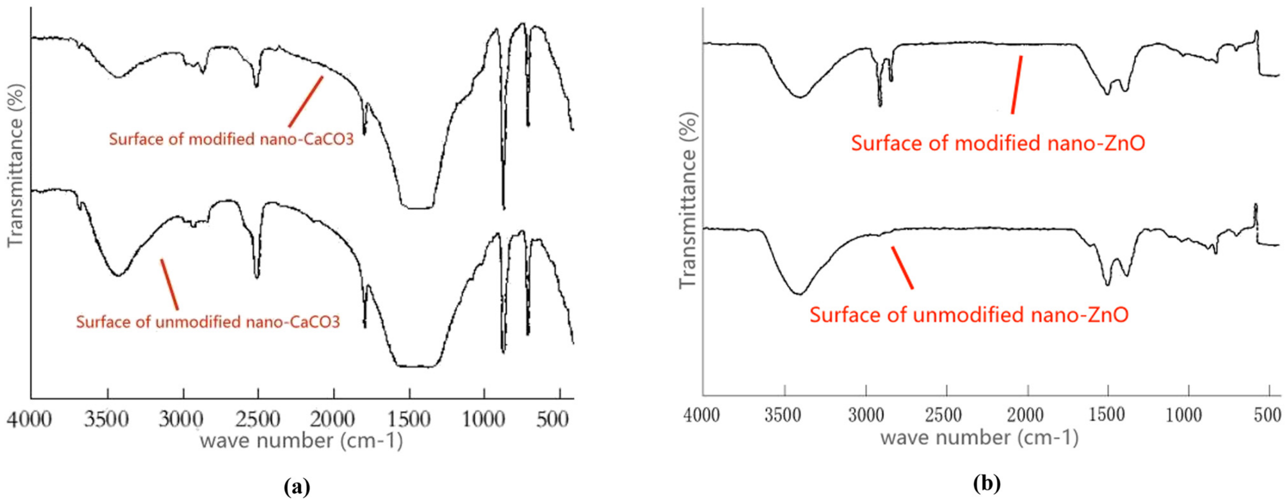

Figure 9: Infrared spectra of modification effect of nanomaterials: (a) IR spectra before and after surface modification of nano-CaCO$_3$ and (b) IR spectra before and after surface modification of nano-ZnO.

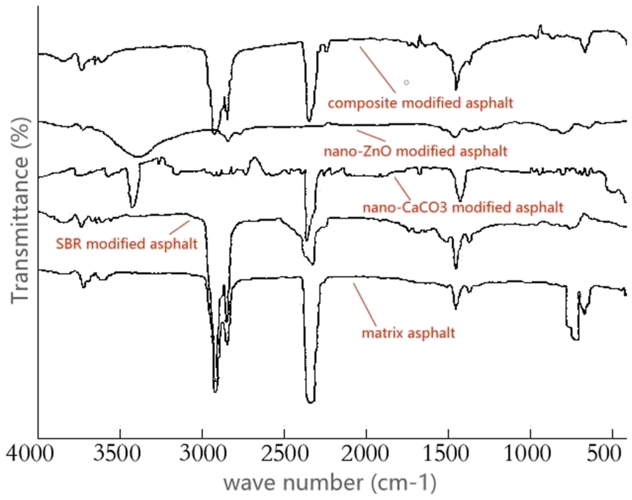

Figure 10: Infrared spectra of five types of asphalt.

to the effect of shear, but it cannot be completely dissolved in it, just is filled in the asphalt in the state of elastic particles, so the surface looks a bit uneven. Nevertheless, the blending effect of SBR and matrix asphalt is still good.

4.6.5 Morphology characterization of nanomaterials/SBR composite-modified asphalt

When the composite-modified asphalt is amplified 5,000 times as shown in Figure 8(a), the shear effect of modifiers mixed together is better than that of nanomaterial alone. The composite-modified asphalt is amplified 20,000 times as shown in Figure 8(b). It is obvious that the three materials are basically completely fused with asphalt. Compared with the three materials alone, the interface layer of the composite-modified asphalt cannot be seen, which is the result of the interaction of the three materials. The network structure formed by nano-CaCO$_3$ and nano-ZnO combined with the filling of SBR particles makes the stability of this structure better than before and the connection between modifiers and matrix asphalt smooth, which is also the reason for the better overall properties of composite-modified asphalt.

4.7 Analysis of Fourier infrared spectrum

According to the test requirement in 3.7, the modification effect of nanomaterials surface coupling agent can be analyzed, and the microscopic analysis of single modified asphalt and composite-modified asphalt can be carried out. Finally, the reaction process in the preparation of modified asphalt is obtained.

4.7.1 Analysis of modification effect of nanomaterials

It can be seen from Figure 9(a) that (1) the absorption peak of nano-CaCO$_3$ before surface modification at 1,476/cm in the spectrum is due to the stretching vibration of C–O bond in CO_3^{2-}. The absorption peak at 2,497/cm is due to the bending vibration of C–O bond in CO_3^{2-}. (2) After the surface of nano-CaCO$_3$ is modified, a new peak appeared at 2,889/cm, which is caused by the stretching vibration and bending vibration of methylene (–CH2–) in coupling agent. Therefore, the chemical bonds in silane coupling agent (KH-550), which is used to modify nano-$CaCO_3$, have been linked to the surface of nano-$CaCO_3$.

It can be seen from Figure 9(b) that (1) the characteristic absorption peak of –OH at 3,450/cm is corresponding to the nano-ZnO before surface modification, and the absorption peak at 503/cm is caused by the stretching vibration of Zn–O bond. (2) Because of the stretching vibration of meth (–CH3) and methylene (–CH2–) in coupling agent, the surface-modified nano-ZnO produced new peaks at 2,784 and 2,910/cm. Therefore, it shows that the surface of nano-ZnO is introduced into the corresponding group of aluminates coupling agent, and they play a good role together.

4.7.2 Analysis of modified asphalt infrared spectrum

It can be clearly seen from Figure 10 that the peak values of matrix asphalt between 2,300–2,500 and 2,700–3,000/cm may be due to the vibration of C–H in paraffin hydrocarbons and cycloparaffins. The difference between modified asphalt and base asphalt is that the absorption peaks at 2,300–2,500 and 2,700–3,000/cm are gradually weakened, which may be mainly due to the chemical reaction between matrix asphalt and hydroxyl (–OH) in the modifier. By observing the infrared spectrum of nano-$CaCO_3$-modified asphalt and nano-ZnO-modified asphalt, it can be found that there are absorption peaks between 3,300–3,500/cm. However, comparing with the spectrum of composite-modified asphalt, it can be found that the absorption peak disappeared, indicating that the chemical reaction between the surface-treated nanomaterials and the matrix asphalt has been occurred under the action of high-speed shear. There have been no obvious changes between the spectrum of SBR-modified asphalt and matrix asphalt, which shows that modifier SBR mainly occurs due to physical changes.

It can be concluded that in the preparation process of composite-modified asphalt, the chemical reaction is mainly occurred with the surface-modified nanomaterials, and at the meantime, the physical reaction is occurred with SBR polymer materials.

5 Conclusion

(1) The lipophilicity test finally determines that nano-$CaCO_3$ is activated by 6% KH-550 and nano-ZnO is activated by 6% aluminate. The best combination dosage is as follows: 4% nano-$CaCO_3$ + 5% nano-ZnO + 4% SBR. The aging performance of the composite-modified asphalt is reduced by 6.9%; the viscosity is increased by 14.6–23.1%. Compared with the matrix asphalt, the *S* values of the stiffness modulus of the low-temperature performance are reduced, and the decrease ratios are 15.6, 30.5, and 17.3% under three temperature conditions. It can be seen that the high-temperature performance, low-temperature performance, aging performance, and viscosity of composite-modified asphalt are better than those of matrix asphalt.

(2) Through the Fourier infrared spectrum test, it is concluded that the chemical reaction mainly occurs between the composite-modified asphalt and the surface-modified nanomaterials, and the physical change occurs with SBR. Not only the three materials can be uniformly dispersed in asphalt, but also the network structure which is formed by nanomaterials combines with the filling of SBR particles and makes the structural stability of modified asphalt better. The connection of modifiers makes the performance of composite-modified asphalt better.

(3) In the next step, the differential scanning calorimetry test of composite-modified asphalt can be analyzed. In addition, all experiments are carried out under relatively ideal environmental conditions in the laboratory. Therefore, a test road needs to be paved for practical verification to see whether its performance can be fully improved under actual environment conditions.

Funding information: This work was supported by Open Fund Project of Zhengzhou Environmentally Friendly High-Performance Road and Bridge Materials Laboratory: [Grant Number Zhengzhou Science [2018] No. 100]; Key R&D and Promotion of Special Scientific and Technological Research Projects of Henan Province: [Grant Number 182102310028, 182102210061]; Key Scientific Research Projects of Colleges and Universities in Henan Province in 2021: Study on Pavement Performance of Cotton Straw Cellulose-modified Asphalt [Grant Number 21A580004]; Open Fund Project of Henan Province Engineering Technology Research Center for Environment-Friendly and High-Performance Pavement Materials (Henan Science foundation [2020] No. 18).

Author contributions: Z. Li contributed to conceptualization, investigation, project administration, supervision, writing-review, and editing. T. Guo contributed to conceptualization, writing-original draft, supervision, visualization, and investigation. Y. Chen contributed to conceptualization, project administration, supervision, and investigation. Q. Liu contributed to conceptualization, supervision, and writing-original draft. Y. Chen: conceptualization, supervision, and investigation. All authors have accepted responsibility for the entire content of this manuscript and approved its submission.

Conflict of interest: The authors state no conflict of interest.

References

[1] Ma F, Dai JS, Fu Z, Liu J, Dong WH, Huang Z. A new type of crumb rubber asphalt mixture: a dry process design and performance evaluation. Appl Sci. 2020;10(1):372.
[2] Xu YQ, Li RM, Zheng CF. Review on application of nanomaterials in asphalt pavement. J China Foreign Highw. 2021;41(1):206–14.
[3] Zhang HL, Su MM, Zhao SF, Zhang YP, Zhang ZP. High and low temperature properties of nano-particles/polymer modified asphalt. Constr Build Mater. 2016;114:323–32.
[4] Mehmet S, Serdal T, Sebnem K. Examination of hot mix asphalt and binder performance modified with nano silica. Constr Build Mater. 2017;156:976–84.
[5] Dalhat MA, Al Abdul Wahhab HI. Performance of recycled plastic waste modified asphalt binder in Saudi Arabia. Int J Pavement Eng. 2015;18(4):349–57.
[6] Wang J, Cai B, Ma HB. Preparation of nano-materials modified asphalt and the dispersion stabilization mechanism. Acta Pet Sin (Pet Process Sect). 2020;36(4):848–56.
[7] Xu OM, Xiao FP, Han S, Serji NA, Wang ZJ. High temperature rheological properties of crumb rubber modified asphalt binders with various modifiers. Constr Build Mater. 2016;112:49–58.
[8] Li RY, Xiao FP, Serji A, You ZP, Huang J. Developments of nano materials and technologies on asphalt materials – A review. Constr Build Mater. 2017;143:1–16.
[9] Zhao BJ, Zhao SF, Zhang HL, Su MM. Properties and mechanism of composite asphalt modified by nano-$CaCO_3$/SBR. J Chang' an Univ (Nat Sci Ed). 2017;37(5):15–22.
[10] Zhai RX, Ge LB, Li Y. The effect of nano-$CaCO_3$/styrene–butadiene rubber (SBR) on fundamental characteristic of hot mix asphalt. Road Mater Pavement Des. 2020;21(4):1006–26.
[11] Zhang H. Evaluation of pavement performance of nano-ZnO/SBS modified asphalt mixture. J China Foreign Highw. 2016;36(02):289–92.
[12] Zhang C, Wang HN, Yang X. Low-temperature performance of SBS modified asphalt mixture in high altitude and cold regions. Int J Pavement Res Technol. 2019;12(1):33–42.
[13] Liu CC, Lv ST, Jin DZ, Qu FT. Laboratory investigation for the road performance of asphalt mixtures modified by rock asphalt–styrene butadiene rubber. J Mater Civ Eng. 2021;33(3):1–10.
[14] Jin DZ, Qian GP, Bai XP. Progress in nano modified asphalt material. N Chem Mater. 2019;47(12):32–6.
[15] Li ZJ, Yang ZN, Su JQ. Impact of organic modified nano-calcium carbonate on aging resistance of asphalt. Highw. 2018;63(11):259–64.
[16] Yang ZN, Li ZJ, Li S. Effect of nano-$CaCO_3$ on rheological properties of road petroleum asphalt. J China Foreign Highw. 2019;39(4):254–8.
[17] Zhang XB, He XH, Jiang FY. Research progress in preparation and application of doped ZnO nanomaterials. N Chem Mater. 2021;3–5:1–6.
[18] Chen YZ, Chen AJ, Li CJ, Li ZX. Analysis of performance for nano-zno modified asphalt mixture. China J Highw Transp. 2017;30(7):25–32.
[19] Zhu QP. Preparation and properties analysis of asphalt modified by nano-ZnO. Appl Chem Ind. 2019;48(5):1031–4.
[20] Yu HY, Ma T, Wang DW, Wang CH, Lu ST, Zhu XY, et al. Review on China's pavement engineering research 2020. China J Highw Transp. 2020;33(10):1–66.
[21] Wang CH, Chen Q, Guo TT, Li Q. Environmental effects and enhancement mechanism of graphene/tourmaline composites. J Clean Prod. 2020;262(5):1–12.
[22] Chen YZ, Wang Q, Li ZX, Ding SQ. Rhysiological properties of graphene nanoplatelets/rubber crowd composite modified asphalt. Constr Build Mater. 2020;261(5):1–12.
[23] TG E20-2011. Standard test methods of bitumen and bituminous mixtures for highway engineering. Beijing: China Communications Press; 2011.
[24] Yang YQ, Tang XD, Tan XX, Hu XY, Xue JL, Guo B. Pavement performance of colored asphalt concrete modified with silane coupling agent. Highw. 2018;63(7):91–4.
[25] Zhang XH. Study on properties of nano calcium carbonate modified asphalt and its mixture. J Changsha Univ Sci Technol (Nat Sci). 2017:1–57.
[26] Fu Z, Chang XR, Dai JS, Dong WH, Zhou Y. Performance analysis of compound modified asphalt with sebs and crumb rubber based on orthogonal test. Sci Technol Eng. 2021;21(6):2445–51.